Tailoring the Generalized 2D Airy Beam

Junpeng Zheng, Ruhao Zhao, Cong Zhang, Meng Xiang, Gai Zhou, Yi Xu, Songnian Fu, *Senior Member, IEEE*, and Yuwen Qin

***Abstract*—Generalized two-dimensional (2D) Airy beam is a kind of self-accelerating beam with variable initial angle between its two wings, manifested itself as an initial angle determined parabolic trajectory during the free-space propagation. However, the independent and flexible manipulation of both the transverse optical field and longitudinal trajectory of the generalized 2D Airy beam has not been achieved yet which limits its application in the various fields. Herein, we report on tailoring of the propagation properties of the generalized 2D Airy beam based on the catastrophe theory, where analytical expression of its propagation trajectory is derived. In order to clarify the relationship between the transverse optical field distribution and the longitudinal trajectory, we analytically put forward a generation vector, facilitating the tailoring of both longitudinal trajectory and transverse distribution of optical field simultaneously. Consequently, we can effectively generate the generalized 2D Airy beam and precisely manipulate the evolution of its peak intensity. Once the initial and terminal points of trajectory are determined in advance, we can flexibly tailor the trajectory of 2D Airy beam, with the help of corresponding generation vector. Meanwhile, when the longitudinal trajectory is fixed, we can flexibly rotate the transverse optical field distribution of the generalized 2D Airy beam and manipulate its initial angle. Experimental verifications of the manipulation capabilities for the longitudinal trajectory, initial angle, and the rotation of transverse optical field are provided to validate our theoretical results.**

***Index Terms*—Airy beam, transverse optical field, longitudinal trajectory.**

I. Introduction

AIRY beam is a kind of typical self-accelerating beams, as its peak intensity position of transverse optical field varies along with the free-space propagation, leading to a typical curved trajectory [1]. Although an Airy wave package solution to the Schrodinger equation in quantum mechanics was theoretically derived in 1979 [2], it is challenging to experimentally generate the Airy beam and observe its parabolic trajectory, because the ideal Airy beam has an infinite energy. After the introduction of the Gaussian envelope [3], Airy beam has been successfully generated, and attracted worldwide research attentions for high-resolution imaging [4], light bullets [5] and optical signal transmission [6], leveraging by its characteristics of self-healing [7], diffraction-free [8], and self-accelerating [9]. We have briefly compared Airy beams with other non-diffractive beams such as Bessel beams [10]. Since the characteristic of Airy beam enables us to choose flexible link in many application scenarios [7], [11], we focus on the arbitrary manipulation of the generalized 2D Airy beams. A 2D Airy beam with an initial angle of can be successfully generated by the vector synthesis of two orthogonal one-dimensional Airy beams [12]. Both the longitudinal trajectory management [13], [14] and the transverse optical field manipulation [15] of a 2D Airy beam with an initial angle of 90° have been reported, leading to various flexible applications [16]. Recently, the generalized 2D Airy beam with a variable initial angle has been experimentally observed, where its longitudinal trajectory is depended on the initial angle [17]. Although the generalized 2D Airy beam provide more degrees of freedom for optical field manipulation, which has many potential applications in the fields of dynamic Airy imaging [11], particle manipulation [18], and 6 G communications [19], its limited regulation hinders its practical applications. Although, the generation of generalized 2D Airy beams can be synthesized by two 1D Airy beams with the same transverse scale, its transverse optical field is always symmetrically distributed, so that both the transverse optical field and the longitudinal trajectory cannot be manipulated individually. Moreover, the existing generalized 2D Airy beams with more than 90° initial angle propagate along the horizontal-throw trajectory, which is challenging to satisfy above-mentioned applications. When the initial angle of the generalized 2D Airy beam is more than 90°, hyperbolic umbilic catastrophe occurs during its free-space propagation. As a result, the deformed transverse optical field leads to a different trajectory, in contrast with the traditional 2D Airy beams. In such case, the peak intensity evolution cannot be simply estimated by the vector synthesis. Therefore, precisely tailoring the longitudinal trajectory of a generalized 2D Airy beam is highly desired. Meanwhile, the relationship between the transverse optical field distribution and the longitudinal trajectory of the generalized 2D Airy beam is still unclear.

In this submission, we introduce variable transverse scaling for two wings and propose a generation vector to realize an arbitrary manipulation of the generalized 2D Airy beams, including both the longitudinal trajectory and transverse distribution of the

Manuscript received 17 January 2024; revised 27 February 2024; accepted 14 March 2024. Date of publication 19 March 2024; date of current version 1 April 2024. This work was supported in part by the National Natural Science Foundation of China under Grant 62025502, and in part by Guangdong Introducing Innovative and Entrepreneurial Teams of "The Pearl River Talent Recruitment Program" under Grant 2021ZT09X044. This paper was produced by the IEEE Publication Technology Group. They are in Piscataway, NJ. *(Corresponding author: Songnian Fu.)*

Junpeng Zheng and Ruhao Zhao are with the Institute of Advanced Photonics Technology, School of Information Engineering, Guangdong University of Technology, Guangzhou 510006, China.

Cong Zhang, Meng Xiang, Gai Zhou, Yi Xu, Songnian Fu, and Yuwen Qin are with the Institute of Advanced Photonics Technology, School of Information Engineering, Guangdong University of Technology, Guangzhou 510006, China, also with the Key Laboratory of Photonic Technology for Integrated Sensing and Communication, Ministry of Education of China, Guangdong University of Technology, Guangzhou 510006, China, and also with the Guangdong Provincial Key Laboratory of Information Photonics Technology, Guangdong University of Technology, Guangzhou 510006, China (e-mail: songnian@gdut.edu.cn).

Digital Object Identifier 10.1109/JPHOT.2024.3378960

generalized 2D Airy beams. The propagation trajectory of the generalized 2D Airy beam tailored by the proposed generation vector is a 3D general parabolic trajectory that can be flexibly regulated. Moreover, once the longitudinal trajectory is determined, the initial angle of a generalized 2D Airy beam can be flexibly adjusted, together with a rotation of its transverse optical field. The tailoring scheme presented here is general and it can be universally applied to other schemes of Airy beam generation, such as metasurface [20] or electron Airy beams [21].

II. Operation Principle

The generalized 2D Airy beam can be generated by the spatial phase modulation in the frequency domain [14]. An input Gaussian beam is initially phase modulated by a spatial light modulator (SLM), which has been loaded with a specially designed phase pattern. Then, after inverse Fourier transform (IFT) by the lens, a generalized 2D Airy beam can be obtained behind the lens, which can be analytically described as

$$\varphi(x,y) = \prod_{n=1,2} Ai\left(\frac{s_n}{r_n}\right)\exp\left(\alpha\frac{s_n}{r_n}\right) \tag{1}$$

where $n = 1, 2$ represents two 1D Airy optical fields used to form two wings of the generalized 2D Airy optical field, $Ai()$ represents the Airy function, $s_n = (-1)^{n-1}x\cos\frac{\theta}{2} - y\sin\frac{\theta}{2}$ represents the coordinate of two 1D Airy optical fields, $\theta \in [\pi/2, \pi)$ is the initial angle between two wings of the generalized 2D Airy beam, r_n is the arbitrary transverse scale of the generalized 2D Airy beam at the corresponding direction, α is the attenuation coefficient which is determined by the Gaussian envelope used during the experimental generation. Since it has minor impact on the trajectory, for the ease of derivation, we set $\alpha = 0$. Both r_n and θ determine the transverse optical field distribution of the generalized 2D Airy beam.

For the ease of generating a generalized 2D Airy beam, we need to load a designated phase pattern into the SLM. It is well-known that the trajectory of Airy beam can be regulated by modifying the cubic phase pattern. We start our analytical investigation by adding the low order terms on the basis of the commonly-used equation of cubic phase modulation. Thus, the phase pattern to generate the generalized 2D Airy beam is shown in (2).

$$\begin{aligned} T_{SLM} = \exp\Bigg\{ i\Bigg[&\frac{r_1^3 k_{s_1}^3}{3} + q_1 r_1^2 k_{s_1}^2 + p_1 r_1 k_{s_1} \\ &+ \frac{r_2^3 k_{s_2}^3}{3} + q_2 r_2^2 k_{s_2}^2 + p_2 r_2 k_{s_2} \Bigg]\Bigg\}, \\ k_{s_n} = (-1)^{n-1}&\frac{k_x}{2\cos(\theta 2)} - \frac{k_y}{2\sin(\theta 2)} \end{aligned} \tag{2}$$

where $k_x = 2\pi x/(\lambda f)$ and $k_y = 2\pi y/(\lambda f)$ are satisfied. λ is the wavelength of beam, f is the focal length of the lens, q_1, q_2, p_1 and p_2 are the dimensionless variables. As shown in (2), the designated phase pattern includes seven parameters, which can be described by a generation vector $Ph = [r_1, q_1, p_1, r_2, q_2, p_2, \theta]$, where r_1, r_2 and q_1, q_2, p_1, p_2 denotes the curvature and the apex position of the parabolic trajectory, respectively. In the current submission, we use the Fresnel diffraction approximation for the analytical derivation. According to (2), the optical field of the generalized 2D Airy beam can be rewritten as

$$\begin{aligned} \varphi_z = &-\frac{r_1 r_2}{\sin\theta}\int_{-\infty}^{\infty} dk_{s_2}\int_{-\infty}^{\infty}\exp(iV)dk_{s_1}, \\ V = &\frac{r_1^3 k_{s_1}^3}{3} + q_1 r_1^2 k_{s_1}^2 + p_1 r_1 k_{s_1} + s_1 k_{s_1} \\ &+ \frac{r_2^3 k_{s_2}^3}{3} + q_2 r_2^2 k_{s_2}^2 + p_2 r_2 k_{s_2} + s_2 k_{s_2} \\ &+ zk - \frac{z}{2k}\left[k_{s_1}^2 + k_{s_2}^2 + 2k_{s_1}k_{s_2}\left(\sin^2\frac{\theta}{2} - \cos^2\frac{\theta}{2}\right)\right] \end{aligned} \tag{3}$$

The V in (3) is an extension of the hyperbolic umbilical model, according to the catastrophe theory. Catastrophe theory can classify critical points according to potential functions and investigate the characteristic of discontinuous phenomena near various critical points. For the system whose internal functions are unknown, but whose discontinuities have been observed, Catastrophe theory provides a rational mathematical model to describe, classify and systematize the Catastrophe. Therefore, the trajectory of the generalized 2D Airy beam can be obtained by solving (3) according to the classical solution. After solving (3) with catastrophe theory [22], the peak intensity trajectory of the generalized 2D Airy beam can be obtained as shown in (4) shown at the bottom of this page.

Now, it is clear that, the trajectory of a generalized 2D Airy beam can be composed of two orthogonal parabolic curves along X and Y directions. In particular, when either $\theta = \pi/2$ or $r_1 = r_2$ is satisfied, both the phase pattern and the estimated trajectory are the same as the previous analytical results [15], [17]. Therefore, we can predict the propagation trajectory of the generalized 2D Airy beam by (4).

Alternatively, we can arbitrarily set a targeted parabolic trajectory between the initial point and the terminal point, as shown in Fig. 1(a). Then, the corresponding generation vector for calculating the phase pattern can be obtained, according to (4). It is interesting that, even we determine the trajectory, the solution of the generation vector is not unique, indicating various possibilities of manipulating the transverse optical field under a fixed trajectory.

$$\begin{cases} x = \frac{\left(r_1^3 - r_2^3\right)\left(\sin^2\frac{\theta}{2} - 3\cos^2\frac{\theta}{2}\right) - 3r_1 r_2(r_1 - r_2)\left(\sin^2\frac{\theta}{2} - \cos^2\frac{\theta}{2}\right)}{8r_1^3 r_2^3 k^2\cos\frac{\theta}{2}} z^2 - \frac{\left(\frac{q_2}{r_2} - \frac{q_1}{r_1}\right)\cos\frac{\theta}{2}}{k} z + \frac{r_1\left(q_1^2 - p_1\right) - r_2\left(q_2^2 - p_2\right)}{2\cos\frac{\theta}{2}} \\ y = \frac{\left(r_1^3 + r_2^3\right)\left(3\sin^2\frac{\theta}{2} - \cos^2\frac{\theta}{2}\right) - 3r_1 r_2(r_1 + r_2)\left(\sin^2\frac{\theta}{2} - \cos^2\frac{\theta}{2}\right)}{-8r_1^3 r_2^3 k^2\sin\frac{\theta}{2}} z^2 - \frac{\left(\frac{q_2}{r_2} + \frac{q_1}{r_1}\right)\sin\frac{\theta}{2}}{k} z + \frac{r_1\left(q_1^2 - p_1\right) + r_2\left(q_2^2 - p_2\right)}{-2\sin\frac{\theta}{2}} \end{cases} \tag{4}$$

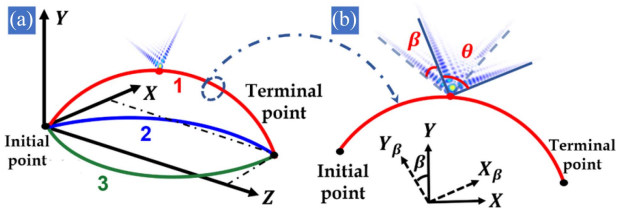

Fig. 1. Schematic of tailoring the generalized 2D Airy beam, including (a) both longitudinal trajectory and (b) transverse optical field, when the variable initial angle θ and the rotation angle β can be arbitrarily.

The flexible manipulation of the generalized 2D Airy beam can be initiated from analyzing its peak intensity trajectory, together with the transverse optical field, based on the catastrophe theory. Generalized 2D Airy beams with different initial angles θ can propagate along the same trajectory, by using various generation vectors according to (4). In such case, the transverse distribution of the optical field can be rotated, as shown in Fig. 1(b). The rotation angle $\beta \leq (\pi - \theta)/2$, is determined by the generation vector of the generalized 2D beam [15]. Finally, both the transverse optical field and the longitudinal trajectory of the generalized 2D Airy beam can be independently tailored.

III. Simulation

In this section, we investigate the generation and manipulation of a generalized 2D Airy beams through numerical simulation by Matlab, so that we can verify the accuracy of the theoretically predicted trajectory in Section II.

A. Tailoring the Trajectory

First, we evaluate the accuracy of the trajectory prediction based on (4). The Gaussian beam is modulated in the frequency domain by the phase pattern calculated by (2), and then the Fourier transform is performed by a lens with a focal length of 100 mm to generate a generalized 2D Airy beam, which can be used to verify the theoretical results.

Generally, if both initial and terminal points of propagation trajectory are fixed, we can obtain various generation vectors to tailor the trajectory of the generalized Airy beam. In order to fully present the generalized 2D Airy beams with various initial angles, we perform a certain rotation of the coordinate, and all results are shown in Fig. 2. As we can see, the initial and terminal points of generalized Airy beams with variable initial angles keep the same and the different generation vectors can be selected to tailor its trajectory. On the other hand, we can tailor the trajectory of the beams, so that they travel along the same transmission path in free-space by the use of the designed generation vectors. The generation vectors Ph used and the simulation results are as shown in Fig. 3. In particular, we can find that, under the condition of $r_1 \neq r_2$, the trajectory of the beam is projected as a general parabola at both X-axis and Y-axis, according to (4) and Fig. 3. Thus, the trajectory manipulation is no longer subject to the limitation of existing generation schemes.

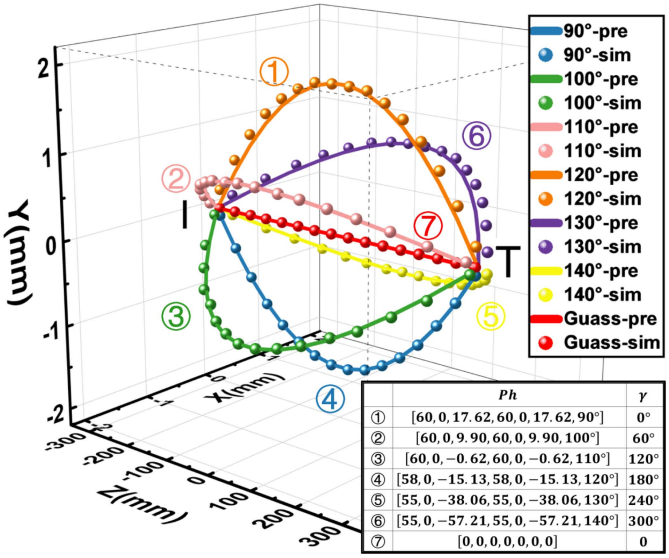

	Ph	γ
①	[60, 0, 17.62, 60, 0, 17.62, 90°]	0°
②	[60, 0, 9.90, 60, 0, 9.90, 100°]	60°
③	[60, 0, −0.62, 60, 0, −0.62, 110°]	120°
④	[58, 0, −15.13, 58, 0, −15.13, 120°]	180°
⑤	[55, 0, −38.06, 55, 0, −38.06, 130°]	240°
⑥	[55, 0, −57.21, 55, 0, −57.21, 140°]	300°
⑦	[0, 0, 0, 0, 0, 0, 0]	0

Fig. 2. Calculated various longitudinal trajectories of the generalized 2D Airy beams with respect to different initial angles. Ph is the generation vectors used and γ is the rotation angle of the coordinate system. The red line represents the Gaussian beam, and other colored lines represent the theoretically predicted trajectories of generalized 2D Airy beams.

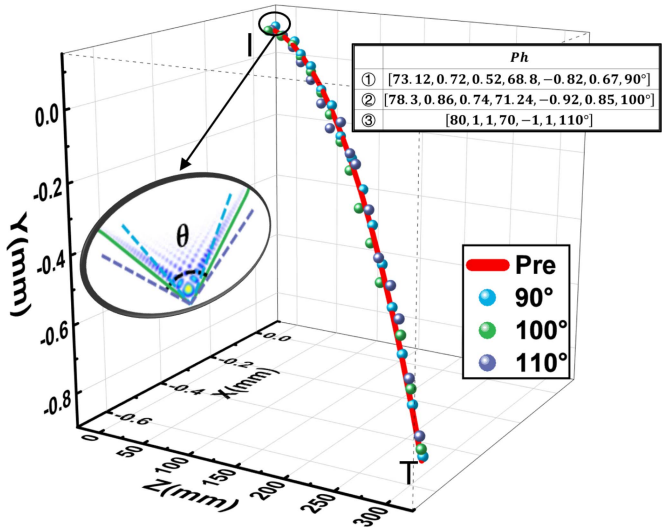

	Ph
①	[73.12, 0.72, 0.52, 68.8, −0.82, 0.67, 90°]
②	[78.3, 0.86, 0.74, 71.24, −0.92, 0.85, 100°]
③	[80, 1, 1, 70, −1, 1, 110°]

Fig. 3. Calculated free-space propagation trajectory of generalized 2D Airy beam with variable initial angles, when various generation vectors are used.

B. Tailoring the Optical Field

We numerically investigate the impact of rotating the transverse optical field of the generalized Airy beam, when the longitudinal trajectory is fixed. As shown in Fig. 4, the transverse optical field distribution can be flexibly tailored, under the condition of a fixed trajectory. Thus, the proposed generation vector is convenient to generate a generalized 2D Airy beam with the capability of rotating its transverse optical field, when the longitudinal trajectory is the same.

C. Beam Quality Monitoring

Next, we verify the advantage of the generalized 2D Airy beams with different initial angles, in comparison with

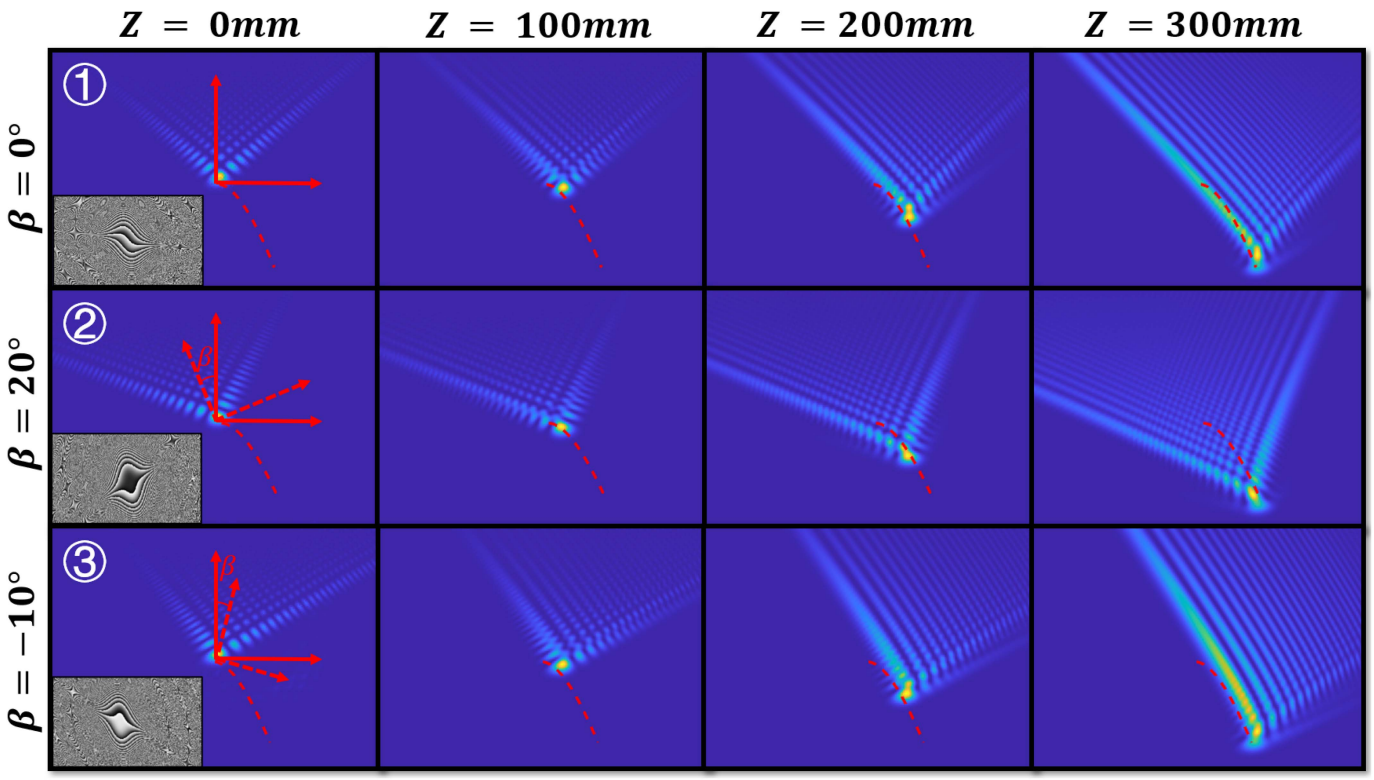

Fig. 4. Calculated free-space propagation results of the generalized 2D Airy beam propagating with different distributions of transverse optical field, when the initial angle θ is 100° and the trajectory is fixed.

traditional 2D Airy beams. It is well known that, the experimentally generated Airy beams with the finite energy will gradually degenerate into a Gaussian beam, after the maximum transverse offset. Then, its peak intensity will no longer propagate along the designated trajectory. It has been identified that, 2D Airy beams with various initial angles have different propagation characteristics [17], indicating that their achievable maximum transverse offsets are different. Thus, we can use the proposed scheme to tailor the generalized 2D Airy beam and monitoring the evolution of beam quality under the same trajectory. The beam quality is evaluated by its peak intensity ratio R

$$R = \frac{P_2}{P_1} \tag{5}$$

where P_1 represents the peak intensity of the main lobe of the transverse optical field, and P_2 represents the peak intensity of the entire optical field, except the main lobe. This metric is focused on the energy proportion of the main lobe for the non-diffracted beam. When $R \geq 1$ is observed, the energy of the main lobe is less than half of the whole energy of the optical field. Consequently, the beam does not preserve its Airy profile anymore. As shown in Fig. 5, under the condition of a fixed trajectory, the traditional 2D Airy beam degenerates after 173 mm free-space propagation, and its maximum transverse offset is about 0.77 mm. However, the self-acceleration characteristics of generalized 2D Airy beams with initial angles of larger than 90° can be enhanced, and its maximum transverse offset also increases with the growing initial angle. By taking generalized

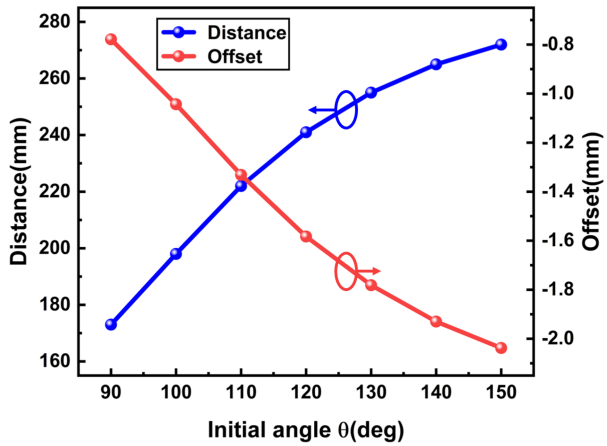

Fig. 5. Simulation results of the generalized 2D Airy beams in the terms of the free-space propagation distance and the maximum transverse offset.

2D Airy beams with initial angles 120° as an example, its free-space propagation can reach 241 mm and the maximum transverse offset can be up to 1.58 mm, which is nearly 105% more than that of a traditional 2D Airy beam.

IV. Experiment

We carry out the experimental verification for the proposed trajectory tailoring scheme, in consistent with the simulation results. Since the manipulation results are almost the same, for

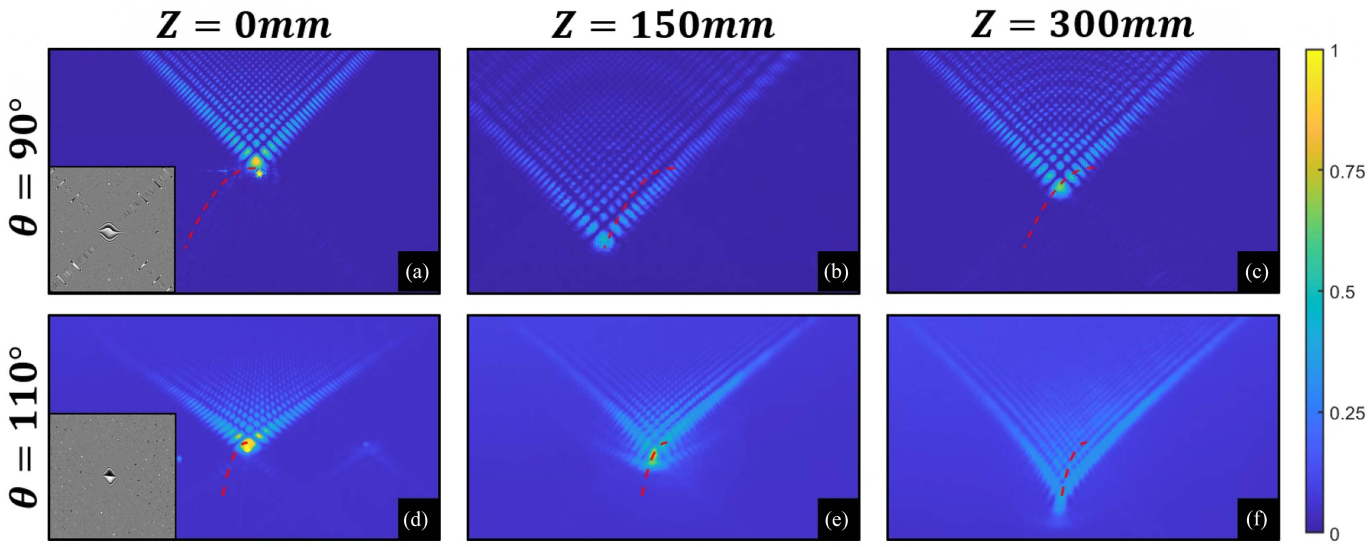

Fig. 6. Experimental free-space propagation results of the generalized 2D Airy beams over the fixed trajectory.

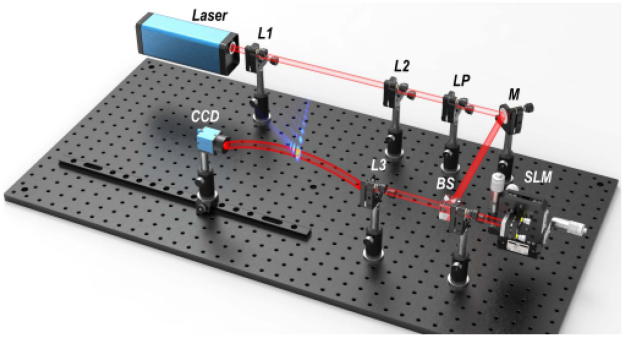

Fig. 7. Schematic of experimental setup. L: Lens, LP: Linear Polarizer, M: Mirror, BS: Beam splitter, SLM: Spatial Light Modulator, CCD: Charge Coupled Device.

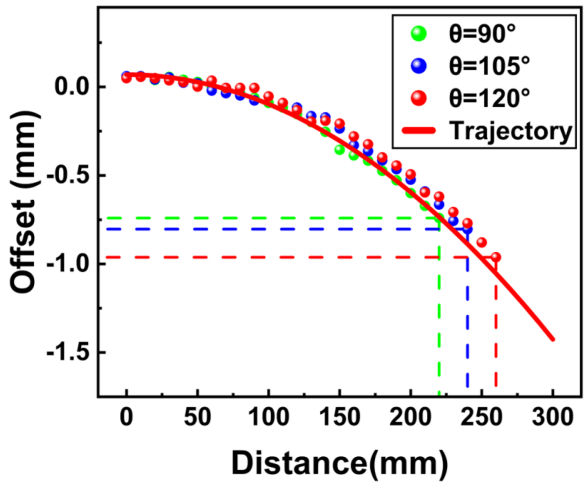

Fig. 8. Experiment results of the enhanced self-accelerating characteristic for the generalized 2D Airy beam.

the ease of presentation, we randomly choose some generation vectors to generate the corresponding beams and compare them with the analytical and simulation results, as shown in Fig. 7. The Gaussian beam from a 633 nm semiconductor laser output is introduced into a 4F system including two lenses of L1 and L2. Then, after the Gaussian beam passes through a linear polarizer (LP) and a beam splitter (BS), it is spatially modulated by a reflective liquid-crystal-on-silicon (LCOS) SLM (PLUTO-2.1 IR-133, HOLOEYE). The SLM has a resolution of 1920 $\times$ 1080 with a pixel spacing of 8 μm. When the lens L3 with a focal length of 100 mm is used after LCOS. The generalized 2D Airy beam can be obtained at the rear focal plane. Subsequently, a CCD (MER2-1220-32U3C, Daheng) is used for recording the intensity profile. When the phase pattern is calculated by the corresponding generation vector and loaded into the LCOS, we start to monitor the peak intensity along the longitudinal direction. Since the transverse optical field distribution and the longitudinal transmission trajectory are linked with the generation vector, various generalized 2D Airy beams can be monitored, as shown in Fig. 6.

In order to experimentally verify the accuracy of the estimated trajectory, we use different generation vectors to tailor the trajectory of generalized 2D Airy beams with initial angles of 90° and 110°, as shown in Fig. 6. The red dashed lines represent the predicted trajectory, which is in good agreement with the peak intensity evolution of the optical field. Fig. 6(a)–(c) is the experimental results of the traditional 2D Airy beam, indicating that (4) is still valid for the traditional 2D Airy beam. Fig. 6(d)–(f) is the experimental results of the generalized 2D Airy beams propagated along the determined trajectory. Thus, we can arbitrarily tailor the trajectory of the generalized 2D Airy beams, with the help of the generation vector. Finally, the enhanced self-accelerating characteristic of the generalized Airy beam is experimentally verified. Under the condition of fixed trajectory, various generalized 2D Airy beams with variable initial angles are experimentally evaluated, as shown in Fig. 8. The achievable maximum transverse offset of the generalized

2D Airy beam does increase with the growing initial angle, in a consistent with the simulation results. The generalized 2D Airy beam with an initial angle of 120° has a maximum transverse offset of 0.96 mm, which is about 30% larger than that of the traditional 2D Airy beam.

V. Conclusion

In summary, We theoretically derive a generation vector to effectively realize the generation and tailoring of the generalized 2D Airy beams. It is shown that, both the transverse optical filed and the longitudinal trajectory of the generalized 2D Airy beam can be independently manipulated, facilitating its application in various scenarios. Meanwhile, experimental verification is presented to consolidate our theoretical results. Specifically, it is experimentally verified that, the generalized 2D Airy beam with an initial angle of 120° has a maximum transverse offset of 0.96 mm, which is about 30% higher than that of the traditional 2D Airy beam under the same trajectory.

References

[1] I. M. Besieris and A. M. Shaarawi, "A note on an accelerating finite energy airy beam," *Opt. Lett.*, vol. 32, pp. 2447–2449, 2007.

[2] M. V. Berry and N. L. Balazs, "Nonspreading wave packets," *Amer. J. Phys.*, vol. 47, pp. 264–267, 1979.

[3] G. A. Siviloglou and D. N. Christodoulides, "Accelerating finite energy airy beams," *Opt. Lett.*, vol. 32, pp. 979–981, 2007.

[4] T. Vettenburg et al., "Light-sheet microscopy using an airy beam," *Nat. Methods*, vol. 11, pp. 541–544, 2014.

[5] P. Panagiotopoulos, D. G. Papazoglou, A. Couairon, and S. Tzortzakis, "Sharply autofocused ring-airy beams transforming into non-linear intense light bullets," *Nat. Commun.*, vol. 4, 2013, Art. no. 2622.

[6] Y. Liang et al., "Image signal transmission with airy beams," *Opt. Lett.*, vol. 40, pp. 5686–5689, 2015.

[7] J. Broky, G. A. Siviloglou, A. Dogariu, and D. N. Christodoulides, "Self-healing properties of optical airy beams," *Opt. Exp.*, vol. 16, pp. 12880–12891, 2008.

[8] I. Kaminer, R. Bekenstein, J. Nemirovsky, and M. Segev, "Nondiffracting accelerating wave packets of Maxwell's equations," *Phys. Rev. Lett.*, vol. 108, 2012, Art. no. 163901.

[9] M. A. Bandres et al., "Accelerating optical beams," *Opt. Photon. News*, vol. 24, no. 6, pp. 30–37, 2013.

[10] S. Pavone, M. Ettorre, M. Casaletti, and M. Albani, "Analysis and design of Bessel beam launchers: Transverse polarization," *IEEE Trans. Antennas Propag.*, vol. 69, no. 8, pp. 5175–5180, Aug. 2021.

[11] Z. Cai et al., "Dynamic airy imaging through high-efficiency broadband phase microelements by femtosecond laser direct writing," *Photon. Res.*, vol. 8, pp. 875–883, 2020.

[12] G. A. Siviloglou, J. Broky, A. Dogariu, and D. N. Christodoulides, "Observation of accelerating airy beams," *Phys. Rev. Lett.*, vol. 99, 2007, Art. no. 213901.

[13] G. A. Siviloglou, J. Broky, A. Dogariu, and D. N. Christodoulides, "Ballistic dynamics of Airy beams," *Opt. Lett.*, vol. 33, pp. 207–209, 2008.

[14] Y. Hu, P. Zhang, C. Lou, S. Huang, J. Xu, and Z. Chen, "Optimal control of the ballistic motion of Airy beams," *Opt. Lett.*, vol. 35, pp. 2260–2262, 2010.

[15] L. Zhu, X. Zhao, C. Liu, S. Fu, Y. Wang, and Y. Qin, "Flexible rotation of transverse optical field for 2D self-accelerating beams with a designated trajectory," *Opto- Electron. Adv.*, vol. 4, 2021, Art. no. 200021.

[16] L. Zhu et al., "Airy beam for free-space photonic interconnection: Generation strategy and trajectory manipulation," *J. Lightw. Technol.*, vol. 38, no. 23, pp. 6474–6480, Dec. 2020.

[17] Y. Liang et al., "Dynamical deformed airy beams with arbitrary angles between two wings," *J. Opt. Soc. Amer. A*, vol. 31, pp. 1468–1472, 2014.

[18] J. Baumgartl, M. Mazilu, and K. Dholakia, "Optically mediated particle clearing using Airy wavepackets," *Nature Photon.*, vol. 2, pp. 675–678, 2008.

[19] J. Zhang et al., "A 6G meta-device for 3D varifocal," *Sci. Adv.*, vol. 9, no. 4, 2023, Art. no. eadf8478.

[20] B. Yu et al., "Polarization-independent highly efficient generation of airy optical beams with dielectric metasurfaces," *Photon. Res.*, vol. 8, pp. 1148–1154, 2020.

[21] N. Voloch-Bloch, Y. Lereah, Y. Lilach, A. Gover, and A. Arie, "Generation of electron airy beams," *Nature*, vol. 494, pp. 331–335, 2013.

[22] M. V. Berry, *Catastrophe Optics: Morphologies of Caustics and Their Diffraction Patterns*, E. Wolf E.d. North-Holland, Amsterdam, The Netherlands: Optics XVII, 1989.